Journal of
Synchrotron
Radiation

ISSN 1600-5775

Received 24 July 2014
Accepted 19 October 2014

X-ray irradiation induces local rearrangement of silica particles in swollen rubber

Yuya Shinohara,[a]* Naoko Yamamoto,[a] Hiroyuki Kishimoto[b] and Yoshiyuki Amemiya[a]

[a]Department of Advanced Materials Science, Graduate School of Frontier Sciences, The University of Tokyo, 5-1-5 Kashiwanoha, Kashiwa, Chiba 277-8561, Japan, and [b]Sumitomo Rubber Industries Ltd, 3-6-9 Wakinohamacho, Chuo, Kobe, Hyogo 651-0072, Japan. *E-mail: yuya@k.u-tokyo.ac.jp

X-ray photon correlation spectroscopy (XPCS) of swollen rubber containing spherical silica nanoparticles is reported. It is shown that irradiation by intense X-rays leads to the breakdown of cross-links, thereby inducing the local rearrangement of silica nanoparticles. This rearrangement process depends on the cross-link density and is characterized by a compressed exponential relaxation with aging behaviour, which resembles a common feature of complex fluids observed with XPCS.

Keywords: X-ray photon correlation spectroscopy; filled rubber.

1. Introduction

The interplay between microscopic structure and bulk viscoelasticity of colloidal suspensions has received considerable attention (Mewis & Wagner, 2012; Sonn-Segev *et al.*, 2014). The presence of nanoparticles in polymeric matrices significantly influences their mechanical and viscoelastic properties (Guth, 1945; Kluppel, 2003; Oberdisse, 2006; Balazs *et al.*, 2006). This so-called reinforcement effect is indispensable for utilizing nanocomposites in daily life, and hence understanding its physical picture has been a subject of research (Witten *et al.*, 1993; Baeza *et al.*, 2013; Nusser *et al.*, 2013; Pérez-Aparicio *et al.*, 2013). So far, a detailed mechanism of the effect considering microscopic structure and dynamics has yet to be rationalized. We thus aim to explore the relationship between its microscopic spatio-temporal structure and bulk viscoelastic and mechanical properties. X-ray photon correlation spectroscopy (XPCS) has been used for elucidating microscopic slow dynamics in hard and soft condensed matter (Leheny, 2012; Sutton, 2008). Speckle patterns observed in XPCS measurements directly reflect the electron-density distribution without averaging, hence is utilized for observing local microscopic dynamics for various systems. When applied to filled rubber, XPCS offers information about the microscopic dynamics of the nanoparticles (Ehrburger-Dolle *et al.*, 2012; Shinohara *et al.*, 2010*a*, 2012).

Most XPCS studies of complex fluids report that the intensity–intensity correlation function, $g^{(2)}(q, t)$, shows a compressed exponential behaviour, $g^{(2)}(q, t) = 1 + \beta|\exp[-(t/\tau)^p]|$, with the exponent p being larger than unity (Cipelletti & Ramos, 2005). Here, τ and β represent the relaxation time and the contrast factor, respectively. As a physical picture of this compressed exponential behaviour, there are two leading hypotheses (Madsen *et al.*, 2010): a continuous-time random walk model (Caronna *et al.*, 2008) and a stress response to the relaxation of local stress model (Bouchaud & Pitard, 2001); still, the physical picture is not clear.

Another common feature observed in XPCS measurements of complex fluids is aging. Systems showing compressed exponential relaxation commonly show an aging behaviour (Bandyopadhyay *et al.*, 2004; Fluerasu *et al.*, 2007). A previous study on the dynamics of nanoparticles in uncross-linked rubber shows that the local stresses accompanying the mixing process of silica and rubber polymers induce this aging behaviour (Shinohara *et al.*, 2010*a*). A recent heterodyne XPCS study of elongated rubber also shows aging behaviour with a compressed exponential relaxation (Ehrburger-Dolle *et al.*, 2012). Aging has been a subject in many systems (Gotze & Sjogren, 1992; Bouchaud *et al.*, 1996) and many studies have been conducted. Dynamical heterogeneity has emerged as a key concept for understanding the peculiar dynamics (Ediger, 2000; Richert, 2002); still a theoretical understanding of the microscopic rheology of suspensions as well as the clarification of the heterogeneous dynamics has yet to be rationalized. To elucidate the microscopic dynamics of colloidal suspensions, we need to build a physical picture of the aging and compressed exponential relaxation behaviours based on experimental results.

Aside from aging of the system, X-ray irradiation onto soft matter is known to induce certain radiation damage. It is recognized that X-ray irradiation significantly influences the dynamics of a system by X-ray radiation damage (Ehrburger-Dolle *et al.*, 2012); this indicates that aging dynamics should be discussed in accounting for the effect of X-ray radiation damage in XPCS measurements.

In this paper we report XPCS of silica nanoparticles in swollen rubber. We have found that X-ray irradiation itself

does affect the XPCS results; aging and compressed exponential behaviour are significantly related to the X-ray irradiation. In the following we report that the aging behaviour in the present system is related to the local rearrangement of particles induced by XPCS measurements themselves.

2. Materials and methods

2.1. Materials

Silica particles (KE-P10, Nippon Shokubai Ltd, Japan) embedded in commercially available styrene-butadiene rubber (SBR1502) were used as the sample, the detailed contents of which are shown in Table 1. Rubber polymer was covalently cross-linked by dicumylperoxide (DCP). The diameter of the silica particles was 1.2×10^2 nm. Phenyltriethoxysilane (KBE103, Shin-Etsu Chemical Co. Ltd) was added, forming the following 'S-samples': S-low, S-mid and S-high; this silane covers the silica particles and its phenyl group may interact with phenyl groups in SBR *via* π–π interactions, thereby coupling the silica particles with rubber polymers. As controls, rubber filled with raw silica particles without silane were also prepared (*i.e.* 'R-samples' R-low, R-mid and R-high). After all of the ingredients were mixed, the samples were heated at 443 K for 12 min, and then formed into a sheet of thickness 1 mm. All of the samples were swollen by using cyclohexanone as solvent for 60 h prior to the X-ray measurements. The swollen samples were sealed in a stainless cell with windows made of polyimide to prevent evaporation of cyclohexanone during the measurements.

2.2. X-ray photon correlation spectroscopy

XPCS measurements were conducted at BL40XU, SPring-8 (Shinohara *et al.*, 2007). Quasi-monochromatic X-rays from a helical undulator were used to produce partially coherent X-rays by inserting a pinhole. An X-ray CCD detector coupled to an X-ray image intensifier (Shinohara *et al.*, 2010*b*) was used for recording speckle images. For each measurement, 1000 images were recorded at 364 ms intervals under continuous X-ray illumination. These images were processed after subtraction of an averaged dark intensity of the CCD detector. All measurements were performed at room temperature. The X-ray flux at the sample position was estimated to be 3×10^{10} photons s^{-1}.

Table 1
Sample code. All numbers represent the weight ratio. DCP stands for dicumulyperoxide. For the SBR and silane, SBR1502 and phenyltrieth-oxysilane were used.

Code	R-low	R-mid	R-high	S-low	S-mid	S-high
SBR	100	100	100	100	100	100
Silica	11.1	11.1	11.1	11.1	11.1	11.1
DCP	0.3	0.5	0.3	0.3	0.5	0.7
Silane				1.1	1.1	1.1
Stearic acid	2.0	2.0	2.0	2.0	2.0	2.0

3. Results and discussion

Fig. 1 shows the mappings of a two-time correlation function of S-low, S-mid and S-high at $q = 0.04\ \mathrm{nm}^{-1}$. The two-time correlation function, which is defined by

$$C(q, t_1, t_2) = \frac{\langle I(q, t_1) I(q, t_2) \rangle}{\langle I(q, t_1) \rangle \langle I(q, t_2) \rangle}, \quad (1)$$

is widely utilized for visualizing temporal evolutions of the dynamics (Sutton *et al.*, 2003). The results clearly show a slowing down of the dynamics, accompanied by temporal heterogeneity of the dynamics characterized by inhomogeneous fluctuation of the scattering intensity along the diagonal. This slowing down can be interpreted either by structural changes of filler aggregates or viscoelastic properties surrounding the nanoparticles. Figs. 2(*a*)–2(*f*) show normalized azimuthally averaged scattering intensity profiles at $t = 0$, 36, 73, 109 and 360 s, where t is the elapsed time since the start of the X-ray exposure. The exposure time was 364 ms. No significant changes during X-ray irradiation were shown. We therefore conclude that the slowing down was not due to structural changes such as aggregation.

To build a physical picture of the slowing down, we compared the temporal evolution of the scattering intensity at $q = 0.04\ \mathrm{nm}^{-1}$ [Fig. 2(*g*)–2(*l*)]. The S-samples did not show any significant decrease in scattering intensity while the R-samples showed a rapid decrease. In the present case the observed scattering intensity originates from the electron density contrast between the rubber and silica particles. The rapid

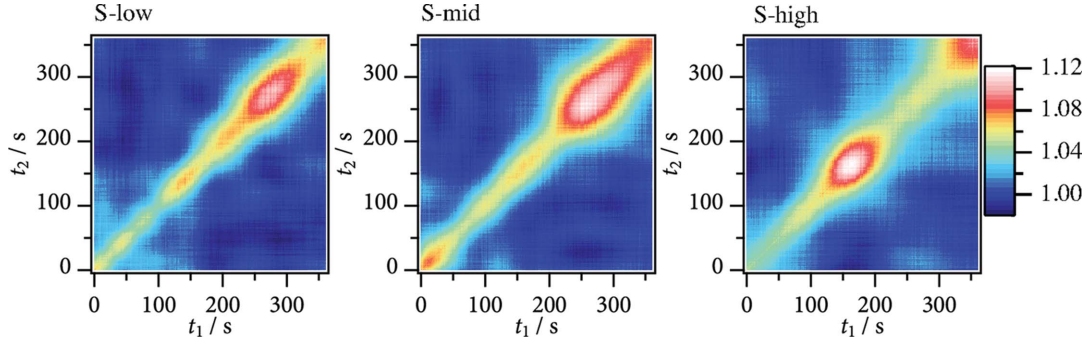

Figure 1
Typical two-time correlation function of S-low, S-mid and S-high at $q = 0.04\ \mathrm{nm}^{-1}$. All figures show a slowing down of the dynamics with inhomogeneous intensity fluctuation along their diagonal. The colour scales represents values.

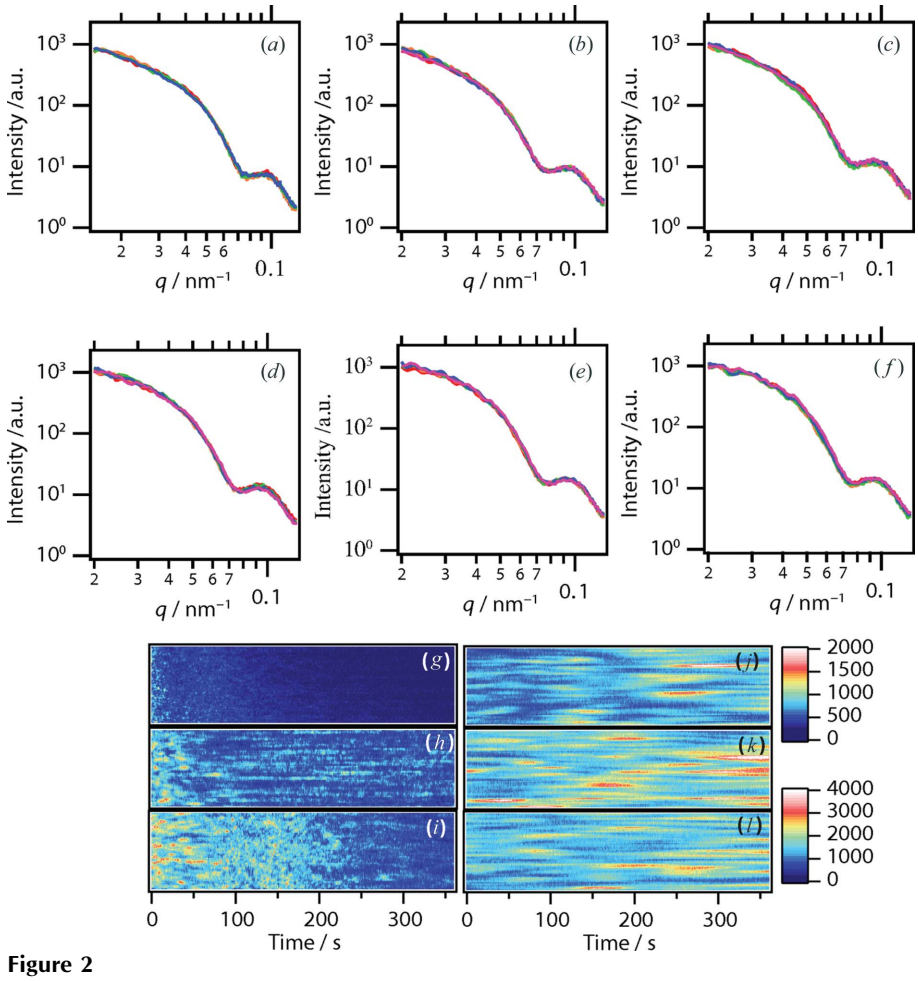

Figure 2
(*a*)–(*f*) Reduced scattering intensity profiles and (*g*)–(*l*) typical example of time evolution of the scattering intensity at $q = 0.04$ nm^{-1}. (*a*, *g*) R-low, (*b*, *h*) R-mid, (*c*, *i*) R-high, (*d*, *j*) S-low, (*e*, *k*) S-mid and (*f*, *l*) S-high. The profiles at $t = 0$, 36, 73, 109 and 360 s are plotted in (*a*)–(*f*); they completely overlap. The upper and lower colour scales represent the intensity of the R-samples and S-samples, respectively.

decrease is thus attributed to the decrease in the number of nanoparticles under X-ray illumination. When another position on the sample was illuminated, the same behaviour was observed; we thus conclude that X-ray irradiation of the R-samples induced a decrease in the number of nanoparticles within the illuminated part of the sample. This decrease is attributed to the breakdown of polymer cross-links due to X-ray irradiation. Prior to the irradiation, a networked structure of cross-linked rubber polymers entangled with the silica nanoparticles, thereby preventing them from escaping from the cages of polymer chains. Once the X-rays are irradiated, the cross-links are broken and the nanoparticles are no longer caged; consequently the nanoparticles disperse among the solution. Further studies concerning the detailed mechanism of radiation damage deserve future work.

For the S-samples, such a drastic decrease in scattering intensity was not observed; this means that the number of nanoparticles did not change in contrast to the case of the R-samples. It is natural to assume that the cross-link structure is the same for the R-samples and the S-samples; therefore it is also natural to consider that the cross-links were similarly broken with the irradiation of X-rays even for the S-samples. Still, the silane covering the nanoparticles interacted with rubber polymers *via* π–π interactions in the S-samples, and we speculate that the silica nanoparticles acted as cross-links that were not broken by the X-ray irradiation and/or were reversibly recovered after the breakdown. Based on this speculation, the silica nanoparticles of the S-samples were trapped within the illuminated parts; this certainly explains the difference observed for the R- and S-samples.

To gain insight into the detailed dynamics of the S-samples, intensity correlation functions are calculated at several stages. Fig. 3(*a*) shows typical time-correlation functions at an initial stage of X-ray irradiation ($0\ \text{s} \leq t \leq 109$ s). They are fitted to a single exponential function with the exponent p being larger than unity as shown in Figs. 3(*b*)–3(*d*). This compressed exponential relaxation behaviour agrees with those observed in jammed or dense systems (Guo *et al.*, 2009; Srivastava *et al.*, 2009; Ehrburger-Dolle *et al.*, 2012; Chen *et al.*, 2013; Ruta *et al.*, 2013). The q-dependence of the relaxation time τ shows a $\tau \simeq q^{-0.5}$ behaviour while uncertainty of data in the low-q region is large owing to the limited number of pixels used for data reduction. The $\tau \simeq q^{-0.5}$ behaviour is observed for all of the systems containing silane at each stage of aging. This scaling shows a striking difference from those observed in many systems showing a compressed exponential behaviour, in which the q-dependence of τ is expressed by $\tau \simeq 1/q$. This scaling is explained within the context of local deformation of the network induced by syneresis (Cipelletti *et al.*, 2003; Cipelletti & Ramos, 2005). The $\tau \simeq q^{-0.5}$ dependence has been observed for thermo-reversible colloidal gel systems (Fluerasu *et al.*, 2007; Solomon & Varadan, 2001), where the scaling is attributed to the disaggregation of the cluster. Based on the above results, we introduce the parameter $a_\text{p} = 1/(q\tau^2)$, which has dimensions of acceleration, by averaging over the whole q-range at each stage. Fig. 4 shows the dependence of a_p on the weight ratio of the cross-linker (DCP). When the weight ratio of the cross-linker is small, a_p initially shows a high value, followed by a rapid decrease with time. At a later stage, a_p shows almost the same value for all of the samples. It is reasonable to assume that the mass of particles does not depend on the amount of cross-linker; thus the behaviour of a_p reflects the intensity of the forces between the particles, thereby being used as a measure of the degree of dynamics.

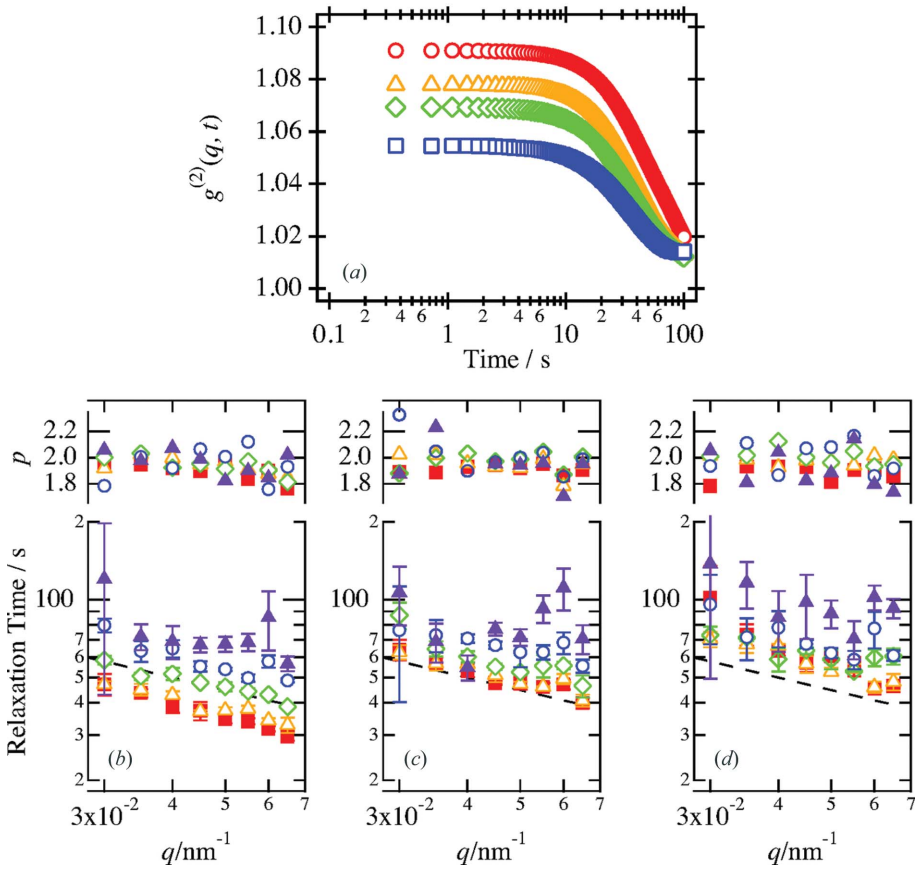

Figure 3
(*a*) Time-correlation function of S-low at q = 0.03 nm^{-1} (circles), q = 0.04 nm^{-1} (triangles), q = 0.05 nm^{-1} (diamonds) and q = 0.06 nm^{-1} (squares). Data for 0 s $\leq t \leq$ 109 s were used to reduce the aging effect. (*b*–*d*) Dependence of relaxation time τ and exponent p on q: S-low (*b*), S-mid (*c*) and S-high (*d*). The dashed line shows $\tau \simeq q^{-0.5}$. The symbols represent the start time used for the analyses: 0 s (squares), 55 s (open triangles), 110 s (diamonds), 164 s (circles) and 219 s (closed triangles).

Based on these results, we propose a physical picture explaining the temporal evolution of the dynamics and the peculiar q-dependence of the relaxation time for the system. As discussed above, the breakdown of cross-links upon X-ray irradiation was observed for the R-samples. It is natural to assume that the X-ray irradiation to the system containing silane also leads to the breakdown of cross-links, thereby resulting in local structural changes. Since no change was observed in terms of the circularly averaged scattering intensity profiles (Fig. 2), it is confirmed that any significant aggregation of silica particles induced by X-ray irradiation is absent for our system; still, the local structural changes such as the breakdown of cross-links induces local rearrangements of silica particles while keeping their averaged configuration. This local rearrangement causes the increase in acceleration of silica particles through the increase in forces upon the particles. When the cross-link density is low (R-low and S-low), the breakdown of cross-links sharply occurs, thereby leading to drastic changes in the configuration of the nanoparticles; the nanoparticles disperse in the absence of silane while the rearrangement occurs in the presence of silane. Consequently, the values of a_p in S-low show a high value at the initial stage of measurement, as shown in Fig. 4. When the cross-link density is large, the time required for the breakdown of cross-links over the whole region becomes large, as confirmed for the R-samples by Fig. 2; as a result, the breakdown of cross-links gradually proceeds. Consequently, the increase of local stress gently proceeds when the cross-link density is high. In summary, (i) the dynamics observed in the present XPCS measurements reflect the local rearrangement of nanoparticles, which is induced by the breakdown of cross-links due to the X-ray irradiation itself, and (ii) the degree of rearrangement is strongly affected by the cross-link density. This picture is supported by the fact that the systems show $\tau \simeq q^{-0.5}$ behaviour. In previous studies of colloidal gels (Fluerasu *et al.*, 2007; Solomon & Varadan, 2001), $\tau \simeq q^{-0.5}$ behaviour is explained as the disaggregation of clusters. If the local rearrangement of nanoparticles is induced by the breakdown of cross-links, its dynamics should resemble those of disaggregation of clusters. This simple speculation does not rule out the possibility that another mechanism such as syneresis-induced network deformation may contribute to the dynamics, but the conclusion requires further investigation and deserves future work.

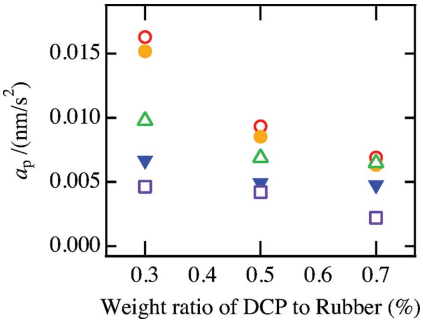

Figure 4
Dependence of a_p on the weight ratio of DCP to rubber. For each stage, data over a period of 109 s were analyzed. The start time used for the analyses was 0 s (open circles), 55 s (closed circles), 110 s (open triangles), 164 s (closed triangles) and 219 s (squares).

As noted above, many systems to which XPCS has been substantially applied show aging dynamics with a compressed exponential relaxation behaviour. The dynamics have been analyzed in a way such that the peculiar dynamics originate from inherent properties of the sample, sample preparation processes or mechanical responses to external fields such as shear. The present study clarifies that X-ray irradiation itself induces similar dynamics for specific samples. Radiation

damage on the sample in XPCS measurements has been widely recognized; the total exposure time for a specific part of the sample is limited to reduce the damage. Still, radiation damage is usually recognized through changes in the scattering intensity profiles, as in the R-samples for the present study. However, even if there is no obvious change in the scattering intensity profiles, the dynamics suffer from the radiation damage as shown in this study. Great care must be taken when utilizing XPCS as a tool for elucidating the complex dynamics of soft matter.

4. Conclusion

The temporal evolution of the dynamics of silica nanoparticles has been observed with XPCS. The changes in dynamics are attributed to the breakdown of cross-links induced by X-ray irradiation. The present study underlines the necessity of the recognition that XPCS sometimes influences the dynamics of a system; still, it demonstrates the usefulness of XPCS for elucidating the detailed dynamics of nanocomposites. Further studies on the effect of interactions between particles and polymers are planned for future experiments.

The XPCS and SAXS experiments were conducted under the approval of the SPring-8 Proposal Advisory Committee (proposal Nos. 2011B1131, 2012A1121, 2012B1103 and 2012B1809). Preliminary SAXS experiments were performed at the Photon Factory under the approval of the Photon Factory Program Advisory Committee (proposal No. 2010G526). This work is partially supported by the Japan Society for the Promotion of Sciences KAKENHI (proposal No. 24710092) and the Photon and Quantum Basic Research Coordinated Development Program from the Ministry of Education, Culture, Sports, Science and Technology, Japan. The authors thank the experimental support from A. Watanabe and I. Ichiro (University of Tokyo) and K. Aoyama and N. Ohta (JASRI/SPring-8).

References

Baeza, G. P., Genix, A.-C., Degrandcourt, C., Petitjean, L., Gummel, J., Schweins, R., Couty, M. & Oberdisse, J. (2013). *Macromolecules*, **46**, 6621–6633.

Balazs, A. C., Emrick, T. & Russell, T. P. (2006). *Science*, **314**, 1107–1110.

Bandyopadhyay, R., Liang, D., Yardimci, H., Sessoms, D. A., Borthwick, M. A., Mochrie, S. G. J., Harden, J. L. & Leheny, R. L. (2004). *Phys. Rev. Lett.* **93**, 228302.

Bouchaud, J.-P., Cugliandolo, L., Kurchan, J. & Mézard, M. (1996). *Physica A*, **226**, 243–273.

Bouchaud, J.-P. & Pitard, E. (2001). *Eur. Phys. J. E*, **6**, 231–236.

Caronna, C., Chushkin, Y., Madsen, A. & Cupane, A. (2008). *Phys. Rev. Lett.* **100**, 055702.

Chen, S. W., Guo, H., Seu, K. A., Dumesnil, K., Roy, S. & Sinha, S. K. (2013). *Phys. Rev. Lett.* **110**, 217201.

Cipelletti, L. & Ramos, L. (2005). *J. Phys. Condens. Matter*, **17**, R253–R285.

Cipelletti, L., Ramos, L., Manley, S., Pitard, E., Weitz, D. A., Pashkovski, E. E. & Johansson, M. (2003). *Faraday Discuss.* **123**, 237–251.

Ediger, M. D. (2000). *Annu. Rev. Phys. Chem.* **51**, 99–128.

Ehrburger-Dolle, F., Morfin, I., Bley, F., Livet, F., Heinrich, G., Richter, S., Piché, L. & Sutton, M. (2012). *Macromolecules*, **45**, 8691–8701.

Fluerasu, A., Moussaïd, A., Madsen, A. & Schofield, A. B. (2007). *Phys. Rev. E*, **76**, 010401.

Gotze, W. & Sjogren, L. (1992). *Rep. Prog. Phys.* **55**, 241–376.

Guo, H., Bourret, G., Corbierre, M. K., Rucareanu, S., Lennox, R. B., Laaziri, K., Piche, L., Sutton, M., Harden, J. L. & Leheny, R. L. (2009). *Phys. Rev. Lett.* **102**, 075702.

Guth, E. J. (1945). *J. Appl. Phys.* **16**, 20.

Kluppel, M. (2003). *Adv. Polym. Sci.* **164**, 1–86.

Leheny, R. L. (2012). *Curr. Opin. Colloid Interface Sci.* **17**, 3–12.

Madsen, A., Leheny, R. L., Guo, H., Sprung, M. & Czakkel, O. (2010). *New J. Phys.* **12**, 055001.

Mewis, J. & Wagner, N. (2012). *Colloidal Suspension Rheology*. Cambridge University Press.

Nusser, K., Schneider, G. J. & Richter, D. (2013). *Macromolecules*, **46**, 6263–6272.

Oberdisse, J. (2006). *Soft Matter*, **2**, 29–36.

Pérez-Aparicio, R., Vieyres, A., Albouy, P.-A., Sanséau, O., Vanel, L., Long, D. R. & Sotta, P. (2013). *Macromolecules*, **46**, 8964–8972.

Richert, R. (2002). *J. Phys. Condens. Matter*, **14**, R703–R738.

Ruta, B., Baldi, G., Monaco, G. & Chushkin, Y. (2013). *J. Chem. Phys.* **138**, 054508.

Shinohara, Y., Imai, R., Kishimoto, H., Yagi, N. & Amemiya, Y. (2010*b*). *J. Synchrotron Rad.* **17**, 737–742.

Shinohara, Y., Kishimoto, H., Maejima, T., Nishikawa, H., Yagi, N. & Amemiya, Y. (2007). *Jpn. J. Appl. Phys.* **46**, l300–L302.

Shinohara, Y., Kishimoto, H., Maejima, T., Nishikawa, H., Yagi, N. & Amemiya, Y. (2012). *Soft Matter*, **8**, 3457–3462.

Shinohara, Y., Kishimoto, H., Yagi, N. & Amemiya, Y. (2010*a*). *Macromolecules*, **43**, 9480–9487.

Solomon, M. J. & Varadan, P. (2001). *Phys. Rev. E*, **63**, 051402.

Sonn-Segev, A., Bernheim-Groswasser, A., Diamant, H. & Roichman, Y. (2014). *Phys. Rev. Lett.* **112**, 088301.

Srivastava, S., Kandar, A. K., Basu, J. K., Mukhopadhyay, M. K., Lurio, L. B., Narayanan, S. & Sinha, S. K. (2009). *Phys. Rev. E*, **79**, 021408.

Sutton, M. (2008). *C. R. Phys.* **9**, 657–667.

Sutton, M., Laaziri, K., Livet, F. & Bley, F. (2003). *Opt. Express*, **11**, 2268–2277.

Witten, T. A., Rubinstein, M. & Colby, R. H. (1993). *J. Phys. II*, **3**, 367–383.